Check for updates

View Article Online
View Journal

Metallomics

Integrated biometal science

Accepted Manuscript

This article can be cited before page numbers have been issued, to do this please use: L. Tabrizi and F. Abyar, *Metallomics*, 2020, DOI: 10.1039/C9MT00304E.

This is an Accepted Manuscript, which has been through the Royal Society of Chemistry peer review process and has been accepted for publication.

Accepted Manuscripts are published online shortly after acceptance, before technical editing, formatting and proof reading. Using this free service, authors can make their results available to the community, in citable form, before we publish the edited article. We will replace this Accepted Manuscript with the edited and formatted Advance Article as soon as it is available.

You can find more information about Accepted Manuscripts in the Information for Authors.

Please note that technical editing may introduce minor changes to the text and/or graphics, which may alter content. The journal's standard Terms & Conditions and the Ethical guidelines still apply. In no event shall the Royal Society of Chemistry be held responsible for any errors or omissions in this Accepted Manuscript or any consequences arising from the use of any information it contains.

ROYAL SOCIETY OF CHEMISTRY

rsc.li/metallomics

View Article Online
DOI: 10.1039/C9MT00304E

Significance to metallomics

Chlorambucil is a famous anticancer drug for some types of cancer. Also, the Pt-based drugs of chlorambucil have been reported as potent anticancer drugs for different cancer cell lines. However, reports on gold(III) complexes with chlorambucil are scanty. Therefore, in the present work, cyclometalated gold(III) complex supported by chlorambucil coupled with phenylpyridine and the hybrid of vitamin B1 with dithiocarbamate as water-soluble complex is reported with the aim of introducing a new and efficient anticancer drug for mechanistic studies in colon and breast cancer for TrRx targets in the cell death pathways.

Published on 03 March 2020. Downloaded by University of Canterbury - Christchurch on 3/3/2020 12:19:07 PM.

Metallomics Accepted Manuscript

View Article Online
DOI: 10.1039/C9MT00304E

Published on 03 March 2020. Downloaded by University of Canterbury - Christchurch on 3/3/2020 12:19:02 PM.

Conjugation of Gold (III) Complex with Vitamin B1 and Chlorambucil Derivatives: Anticancer Evaluation and Mechanistic Insights

Leila Tabrizi [*a], Fatemeh Abyar[*b]

[a] School of Chemistry, National University of Ireland, Galway, University Road, Galway, H91 TK33, Ireland.

[b] Department of Chemical Engineering, Faculty of Engineering, Ardakan University, P.O. Box 184, Ardakan, Iran.

Abstract

The synthesis of a novel class of cyclometalated gold(III) complex supported by chlorambucil coupled with phenylpyridine (CHL-N^C) and the hybrid of vitamin B1 with dithiocarbamate (B1-DTC) with formula $[(CHL\text{-}N\hat{}C)Au^{III}(B1\text{-}DTC)](Cl_2)$, **1**, has been synthesized and fully characterized using different techniques, including multinuclear NMR, mass spectrometry, as well as elemental analysis. This complex is water-soluble and stable in biological environment. This new complex offers a new scaffold to explore biological properties of gold(III) complex as anticancer drug. Antiproliferative activities of the complex **1** and free ligands against the breast and colon cancer cells showed auspicious results with IC_{50} in the micromolar range for complex **1** and more active than cisplatin and free ligands with the selectivity over normal epithelial cells, MRC-5. The DNA binding and inhibition of thioredoxin reductase of complex **1** were studied and compared with the molecular docking results. Moreover, the Au cellular uptake and apoptosis of this new complex were investigated.

Keywords: Chlorambucil, Vitamin B1, Gold (III) Complex, Cytotoxicity, Thioredoxin Reductase.

Metallomics Accepted Manuscript

View Article Online
DOI: 10.1039/C9MT00304E

Published on 03 March 2020. Downloaded by University of Canterbury - Christchurch on 3/3/2020 12:19:02 PM.

1. Introduction

The discovery of the anticancer properties of cisplatin opened the use of metallodrugs in cancer research. [1-6] The gold (I)/(III) complexes have been extensively considered as anticancer effects in vitro and in vivo. [7-9] Gold (I)/(III) complexes have the different mechanisms of action with inhibition of the enzyme thioredoxin reductase (TrxR), poly(adenosine diphosphate (ADP)-ribose) polymerase 1 (PARP-1), reactive oxygen species (ROS) generation, proteasome inhibition, DNA interaction, and kinases alteration. [10-16] These different modes of action support gold complexes to use as effective cytotoxic agents against cancer cells for multidrug-resistant tumor cells. [9]

Cyclometallated gold(III) with (C^N), (N^N^C) or (C^N^C) ligands has been revealed the activities up to the low-micromolar range. [17-20] Mono-cyclometallated (C^N)Au(III) complexes have performed mainly remarkable as a result of the large groups of (C^N) ligands accessible, comprising derivatives of N,N-dimethylbenzylamine, phenylpyridine, benzylpyridine, iminophosphorane. [21-24] These cyclometalation approaches are acquiescent to the coordination of biologically significant or ancillary donor ligands for modification and developed activity. [9,25-28]

Dithiocarbamate (DTC) ligands are also famous for stabilizing Au(III) center. There are some reports in the literature that gold (III) dithiocarbamate complexes showed the effective in vitro anticancer activity. [29-31] The connotation of (C^N) cyclometallated ligands with dithiocarbamates ligands have been discovered in Au(III)-based drug candidates by iminophosphorane or phenylpyridine ligands as anticancer agents with IC_{50} values in the low to submicromolar ranges against different human cancer cells. [26, 32-34]

Vitamin B1 (or thiamine) is composed of an aminopyrimidine and a thiazole ring linked by a methylene bridge. There are some reports in the literature for using vitamin B1 or derivatives such as oxythiamine, 2-(α-hydroxybenzyl) thiamine, thiamine monophosphate and thiamine

Metallomics Accepted Manuscript

View Article Online
DOI: 10.1039/C9MT00304E

Published on 03 March 2020. Downloaded by University of Canterbury - Christchurch on 3/3/2020 12:19:02 PM.

pyrophosphate for making Hg, Cd, Zn, Pt, Cu, Co, Mn, and Rh complexes for biological studies and structure analysis. [35-53]

Chlorambucil is a chemotherapy medication to treat some kinds of cancer with Hodgkin's disease, leukemia, lymphoma, and some breast, lung and ovarian cancers. Some struggles have been completed to conjugate the cytotoxic agent chlorambucil to CPPs (cell-penetrating peptides) with the aim of increasing its efficiency. [54-57] Chlorambucil conjugated with Pt-based drugs has been reported as potent anticancer drugs for different cell lines. [58-60]

The gold complex of chlorambucil promises to combine synergistic anticancer activities of the constituents and would most likely be very effective against various types of cancer. However, reports on such complexes are scanty or somewhat unavailable. Recently, we reported the chlorambucil coupled with an alkynyl group was used as a ligand in the synthesis of mononuclear gold(I) complex and heteronuclear titanocene-gold complex for renal cancer. [61] In continuation our work, here we report the chlorambucil coupled with phenylpyridine as new (C^N) cyclometallated ligand (CHL-N^C) in the synthesis of mononuclear gold(III) complex and the hybrid of vitamin B1 with dithiocarbamate (B1-DTC) as ancillary sulfur donor ligand with formula [(CHL-N^C)Au^{III}(B1-DTC)](Cl_2) with the aim of introducing a new and efficient anticancer drug for mechanistic studies in colon and breast cancer.

2. Results and discussion

2.1. Synthesis and characterization

The 4-(4-(bis(2-chloroethyl)amino)phenyl)-N-(2-phenylpyridin-4-yl)butanamide (chlorambucil-phenylpyridine, CHL-N^C) (Scheme 1) was synthesized by coupling the chlorambucil and 4-amino-2-phenylpyridine as described in experimental part and Scheme S1. The sodium dithiocarbamate vitamin B1 (B1-DTC) (Scheme 1) was synthesized by reaction vitamin B1

Metallomics Accepted Manuscript

View Article Online
DOI: 10.1039/C9MT00304E

Published on 03 March 2020. Downloaded by University of Canterbury - Christchurch on 3/3/2020 12:19:02 PM.

hydrochloride and carbon disulfide in the presence of NaOH (Scheme S2). The complex [(CHL-N^C)Au^{III}(B1-DTC)](Cl_2), **1** (Scheme 1) was synthesized by reacting to the CHL-N^C and B1-DTC with Sodium tetrachloroaurate(III) dihydrate (Na[$AuCl_4$]. $2H_2O$) (Scheme S3). The B1-DTC and complex **1** are completely soluble in water, DMF, DMSO, methanol, and ethanol. But CHL-N^C is soluble in DMF, DMSO, methanol, ethanol, acetonitrile, and chloroform.

The CHL-N^C, B1-DTC, and complex **1** were characterized by multinuclear NMR (^{1}H, ^{13}C, and ^{31}P), and mass spectrometry and their high purity were confirmed by elemental analysis (see Figures S1-S9 of the Supporting Information). The obtained signals of ^{1}H and ^{13}C NMR spectra were consistent with the proposed structures of the CHL-N^C, B1-DTC, and complex **1**.

The ESI-MS spectra of compounds showed peaks centered at m/z 456.16 $[M + H]^+$ (CHL-N^C), 375.01 $[M - Na]^-$ (B1-DTC), and 1028.30 $[M - Cl]^+$ (complex **1**) with the typical isotope patterns the same as simulated ones. The H-b of complex **1** appeared at 7.22 ppm in ^{1}H NMR spectrum that shifted from 8.29-8.35 ppm in free ligand CHL-N^C by coordination to Au(III) center. Moreover, the carbon of dithiocarbamate appeared at 210 ppm in ^{13}C NMR spectrum of B1-DTC that shifted to 197 ppm in complex **1**, illustrating the presence of a complex. This significant shielding of the carbon dithiocarbamate in comparison with the free ligand B1-DTC, in agreement with data reported in the literature for the dithiocarbamate compounds. [62]

Metallomics Accepted Manuscript

View Article Online
DOI: 10.1039/C9MT00304E

Published on 03 March 2020. Downloaded by University of Canterbury - Christchurch on 3/3/2020 12:19:02 PM.

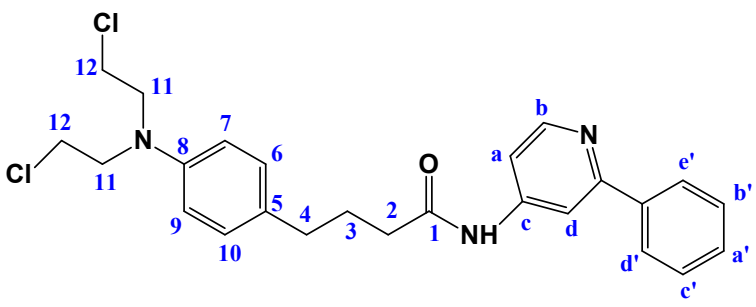

CHL-N^C

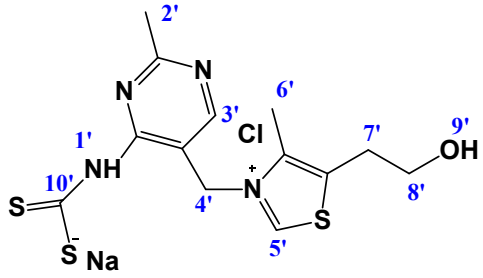

B1-DTC

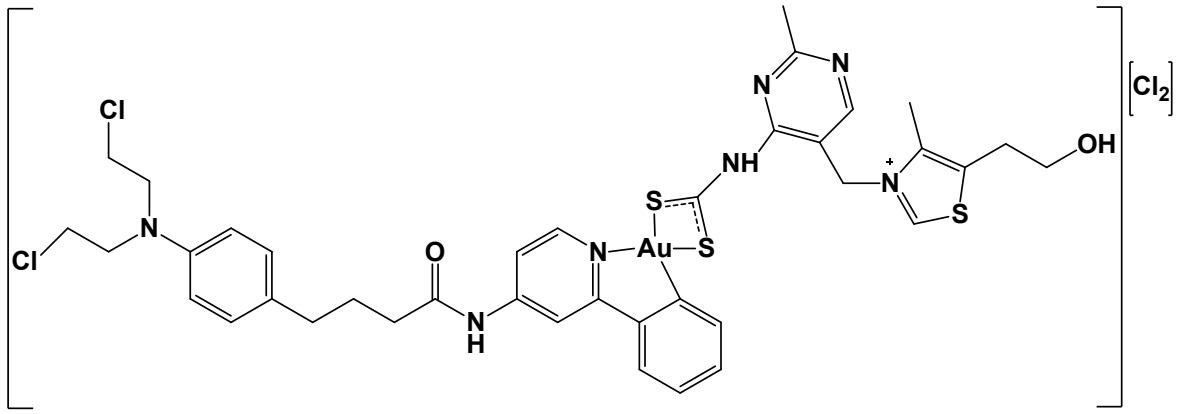

1

Scheme 1. Structures of synthesized compounds.

2.2. Stability of the compounds

The stabilities of the CHL-N^C, B1-DTC, and complex **1** were evaluated in DMSO: PBS buffer (1:99 v/v) for CHL-N^C and PBS buffer for B1-DTC, and complex **1** solution by HPLC-UV at 37 ºC. The results confirmed the purity of the compounds and their stabilities during 72 h (Figure S10). Also, the stability of compounds was studied in DMEM (Dulbecco's Modified Eagle's Medium - high glucose) solution for 72 h (Figure S11). As it is clear, there is no detectable change in retention time during three days, confirming the stability of these compounds under physiological conditions.

Metallomics Accepted Manuscript

View Article Online
DOI: 10.1039/C9MT00304E

Published on 03 March 2020. Downloaded by University of Canterbury - Christchurch on 3/3/2020 12:19:02 PM.

2.3. DNA interaction study

DNA is the main potential biological target for several anticancer metallodrugs. Therefore, the possibility of interaction complex **1** with DNA was explored by multispectroscopic methods and molecular docking simulations. The UV–visible absorption titration of complex **1** in the absence and presence of CT DNA is presented in Figure 1. The hypochromism and redshift were observed by increasing of CT DNA concentration that confirmed the interaction complex **1** with CT DNA. [63] The K_b value of the complex **1** was calculated 7.87×10^{4} M^{-1}. This K_b is in the range of gold(III) complexes that usually interact weak or moderate with DNA. [64]

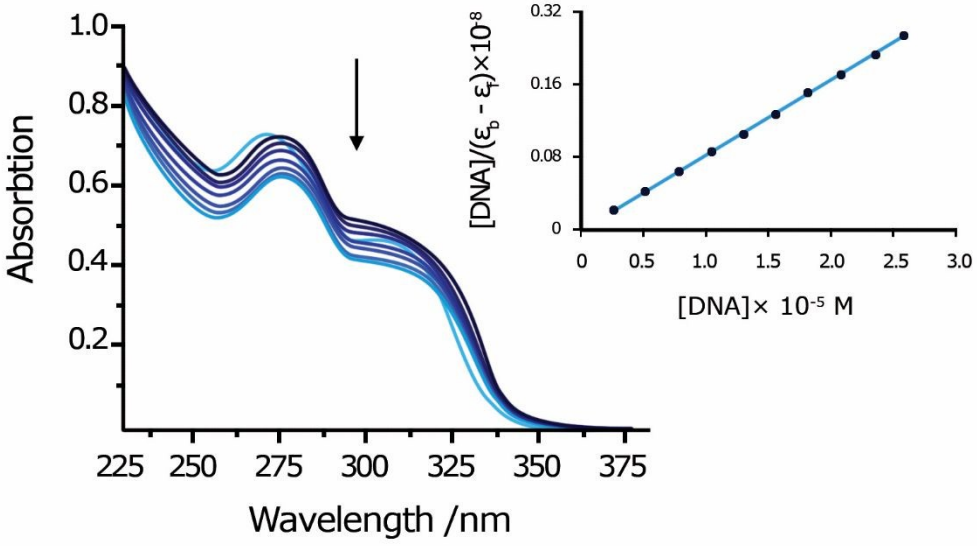

Figure 1. UV–visible spectra of the complex **1** (10 μM) in Tris–HCl buffer by increasing CT DNA concentrations (0-100 μM). Arrow shows that the absorption intensities decrease upon increasing DNA concentration (0-100 μM).

Moreover, the EtBr (ethidium bromide) displacement tests were performed by fluorescence titration (Figure S12) to achieve more information on the mode of DNA interaction. The fluorescence intensity of EB about 600 nm was decreased by increasing the concentration of the

Metallomics Accepted Manuscript

View Article Online
DOI: 10.1039/C9MT00304E

Published on 03 March 2020. Downloaded by University of Canterbury - Christchurch on 3/3/2020 12:19:02 PM.

complex **1** that confirmed the displacement of the DNA bound EB by **1**. The K_q value of the complex **1** was calculated 8.86×10^4 M^{-1}.

Besides, the effect of the complex **1** and Hoechst 33258 (as groove binder) on the viscosity of CT DNA was studied (Figure S13). The relative viscosity of DNA was constant when the concentrations of complex **1** or Hoechst increased. This observation confirmed the groove binding of complex **1** with CT DNA. [63]

2.4. In vitro antiproliferative activity and cellular uptake

Although the ligand CHL-N^C was poorly soluble in an aqueous cell culture medium, but it was soluble enough in the aqueous culture medium with 1% DMSO. However, the B1-DTC and complex **1** were soluble in an aqueous cell culture medium. IC_{50} values for the CHL-N^C, B1-DTC, and complex **1** were then determined on a panel of human cancer cell lines, including breast adenocarcinoma (MCF-7 and MDA-MB-231) and human colon cancer (HCT-116) as well as non-tumorigenic cells human lung fibroblasts (MRC-5). Results were determined using a MTT assay after 72 h of incubation in comparison to cisplatin and auranofin. The results are reported in Table 1.

The free ligands CHL-N^C and B1-DTC were less effective against the MCF-7 and MDA-MB-231 and HCT-116 tumor cell lines ($IC_{50} > 30$ μM). However, the complex **1** showed the high levels of cytotoxicity towards all the tested cell lines. The complex **1** exposed an activity that was 14.5 and 12.41 times higher than that of cisplatin towards MCF-7 and MDA-MB-231 breast cancer with IC_{50} values 1.25 and 2.12 μM, respectively. Moreover, the complex **1** was 12.60 times more active than cisplatin towards HCT-116 colon cancer cells with IC_{50} value 0.43 μM. Moreover, the complex **1** was more active than auranofin against the MCF-7 and HCT-116 tumor cell lines and approximately as the same activity as auranofin against MDA-MB-231 cell

Metallomics Accepted Manuscript

View Article Online
DOI: 10.1039/C9MT00304E

Published on 03 March 2020. Downloaded by University of Canterbury - Christchurch on 3/3/2020 12:19:02 PM.

lines. The complex **1** was also tested against non-tumorigenic cells, MRC-5, which was less active in the healthy cell than cisplatin and auranofin. The calculated SI (selectivity index) value was 21.61 and approximately 11.87 times higher than that obtained for cisplatin.

Table 1. IC_{50} values for compounds in comparison to cisplatin against different human cancer cell lines and healthy MRC-5 cells after 72 h of incubation.

Compounds	IC_{50} (μM) ± SD				SI
	MCF-7	MDA-MB-231	HCT-116	MRC-5	
CHL-N^C	> 30	> 30	> 30	ND	ND
B1-DTC	> 30	> 30	> 30	ND	ND
Complex **1**	1.25 ± 0.03	2.12 ± 0.05	0.43 ± 0.05	82.12 ± 0.10	21.61
Cisplatin	18.21 ± 0.10	26.31 ± 0.21	5.42 ± 0.12	30.27 ± 0.20	1.82
Auranofin	2.89 ± 0.05	2.25 ± 0.15	3.78 ± 0.10	62.43 ± 0.25	21.02

ND: not determined.

With the aim of concluding the relationship concerning cytotoxicity of the compound with intracellular gold accumulation, the uptake of the complex **1** was considered in MCF-7 cancer cells by the graphite furnace atomic absorption spectroscopy (GF-AAS). After treatment by complex **1** (IC_{50} concentration) for 24 h, the intracellular level of gold was detected (192.6 ± 1.4 ng Au/10^6 cells) that is higher than the cellular uptake values of gold (66.2-136.5 ng Au/10^6 cells) in MCF-7 cells by treatment other gold (III) complexes in the literature. [65]

2.5. Inhibition of Thioredoxin Reductase

As TrxR is the main target for gold(III) complexes, complex **1** was verified in vitro for their ability to both cytosolic (TrxR1) and mitochondrial (TrxR2) thioredoxin reductases and compared with auranofin, an well-known TrxR inhibitor and cisplatin as anticancer reference drug. The complex **1** exposed suitable inhibitors of TrxR1 and TrxR2 with IC_{50} values in the

Metallomics Accepted Manuscript

View Article Online
DOI: 10.1039/C9MT00304E

Published on 03 March 2020. Downloaded by University of Canterbury - Christchurch on 3/3/2020 12:19:02 PM.

nanomolar range of concentrations (Table 2). The complex **1** is about 6.43 and 2.56 fold more active than auranofin in inhibiting TrxR1 and TrxR2, respectively. However, complex **1** is more sensitive in inhibiting TrxR1 compare to TrxR2, probably as a result of more accumulation inside cytosolic than mitochondria.

Also, TrxR activity in MCF-7 cells was treated with complex **1** and compared with auranofin and cisplatin under the same experimental conditions (Figure 2) with DTNB (5,5'-dithiobis(2-nitrobenzoic) acid) reduction and the insulin reduction test. The TrxR activities were measured in cell extract with an endpoint method and represented by the percentage of enzyme activity of the lysates from control cells without treatment. [66] In both methods, complex **1** inhibited TrxR activity more than auranofin. However, in the insulin reduction test, complex **1** induced more decrease in TrxR activity.

The glutathione reductase (GR) and glutathione peroxidase (GPx) activities were also tested for complex **1** and auranofin at increasing concentrations (1-100 μM) and IC_{50} values were calculated from the dose-effect curves (Table 2). GR and GPx were affected by complex **1** in less acitivity than auranofin and in the micromolar range of concentration i.e. three orders of magnitude higher than those required for TrxR inhibition. The complex **1** showed the less activity of inhibiting GR and GPx than that observed for auranofin. These results clearly suggest that the complex **1** specially inhibit thioredoxin reductase over the other redox enzymes. The less GR and GPx activity of complex **1** indicated that the C-terminal selenocysteine (Sec) residue in the active site of TrxR is a main target for this compound. [67] These results are in comaprion with other Au(I) complexes that GR and GPx cannot be inhibited by these compounds. [68]

Metallomics Accepted Manuscript

View Article Online
DOI: 10.1039/C9MT00304E

Published on 03 March 2020. Downloaded by University of Canterbury - Christchurch on 3/3/2020 12:19:02 PM.

Table 2. Inhibitory effects of compounds on TrxR1 and TrxR2 (IC_{50}, nM), and TrxR activity (%) in MCF-7 cells.

	TrxR1 IC_{50} (nM)	TrxR2 IC_{50} (nM)	GR IC_{50} (μM)	GPx IC_{50} (μM)
Complex **1**	0.21 ± 0.03	1.45 ± 0.20	52.45 ± 0.18	71.31 ± 0.12
Auranofin	1.35 ± 0.20	3.71 ± 0.13	32.25 ± 0.27	65.13± 0.15
Cisplatin	> 30	> 30	> 100	> 100

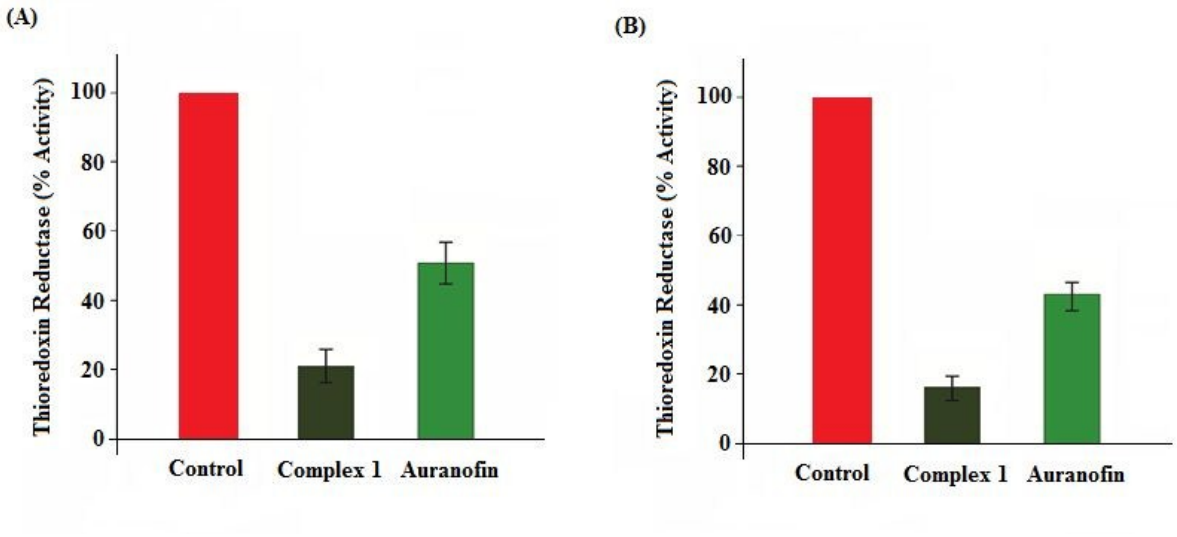

Figure 2. (A) Inhibition of TrxR in the MCF-7 cell lysates by complex **1** and auranofin (A) by DTNB (5,5'-dithiobis(2-nitrobenzoic) acid) reduction (B) with the insulin reduction test. Error bars represent the standard deviation of three independent experiments.

2.6. Induction of apoptosis

To determine the apoptosis effect and the percentage of the necrotic or late apoptotic cells and early apoptotic MCF-7 cells, the cells were treated with 1 μM of complex **1** and cisplatin for 24 h that were analyzed by the annexin V-FITC/PI assay (Figure 3). The complex **1** (1 μM), about 77.02% and 5.38% of the MCF-7 cells were in the early and late apoptotic phase, respectively.

Metallomics Accepted Manuscript

View Article Online
DOI: 10.1039/C9MT00304E

Published on 03 March 2020. Downloaded by University of Canterbury - Christchurch on 3/3/2020 12:19:02 PM.

However, for cisplatin in this concentration, the percentages of the early and late apoptotic phase were to 18.35% and 8.17% in MCF-7. Thus, the complex **1** showed the induced cell death follows mostly through apoptosis.

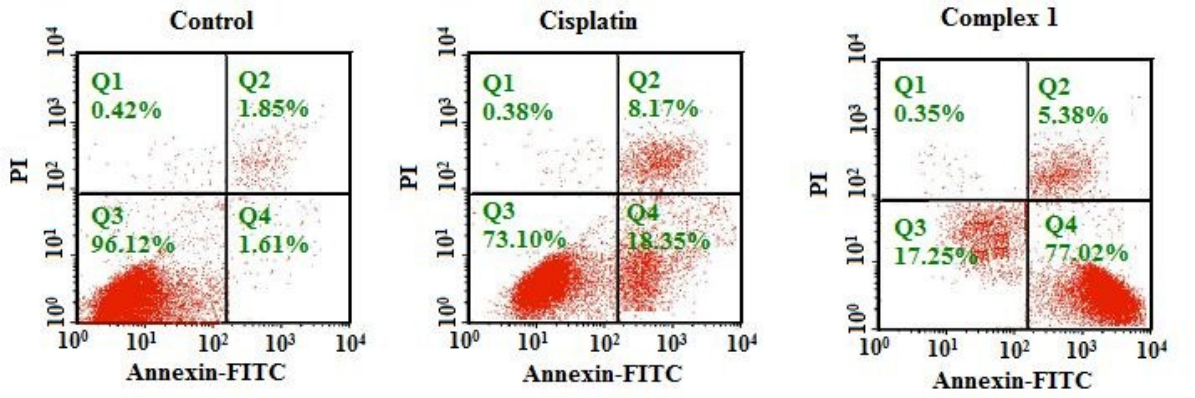

Figure 3. Flow-cytometric analysis of MCF-7 cells after staining with Annexin-V FITC and propidium iodide (PI) for 24 h of incubation with 1 μM of complex **1** and cisplatin (Top right quadrant, dead cells in late stage of apoptosis; bottom right quadrant, cells undergoing apoptosis; bottom left quadrant, viable cells). Representative data from three independent experiments are shown.

2.7. Molecular docking calculations

Molecular docking calculations were carried out as a method to find the appropriate site for the interaction of complex **1** with targets. For molecular docking calculations, structures of different targets were taken from protein data bank (PDB, RCSB website). Ganguly et al [69] have been newly reported crystal structure of human DNA (PDB ID: 5zld) with sequence d ((5'-D(*CP*GP*CP*GP*AP*AP*AP*TP*TP*TP*CP*GP*CP*G)-3'))2. Crystal structure of the human thioredoxin reductase-thioredoxin (TrxR1) with PDB entire: 3QFA [70] and thioredoxin-2 enzyme (TrxR2) with PDB ID: 4O32 [71] were taken from the with the resolution 2.2 and 2.19 Å, respectively. [72] TrxR is a homodimeric flavoprotein crucially involved in the regulation of

Metallomics Accepted Manuscript

View Article Online
DOI: 10.1039/C9MT00304E

Published on 03 March 2020. Downloaded by University of Canterbury - Christchurch on 3/3/2020 12:19:02 PM.

cellular redox homeostasis, growth, and differentiation. Its importance in various diseases makes TrxR a highly interesting drug target. Therefore, investigations on their active sites play an important role in designing drugs and to find inhibition of the TrxR activity.

For the determination of best interaction modes, the pre-molecular docking analyses were done by Hex 8 [73] and Auto Dock 4.2 package [74] for finding the best active site of interaction. Also, the lowest energy structures were selected for future molecular calculations. Then the active site with the highest binding affinity was obtained from pre docking as the initial file in the focus calculations with Autodock 4.2 program. Genetic algorithm (GA) was used to search for finding low energy site of the target with the combined conformation/orientation states. The GA can be done for docking flexible molecules with a number of runs set to 50 into surface targets. [75] The size of the grid box in the focus docking calculations for DNA, TrxR 1 and 2 were set 66*78*66, 82*96*106 and 90*88*88 A^{o3} the x, y and z directions, respectively also the binding sites were computed by grid point spacing of 0.375 Å for all calculations. Other molecular docking procedure's parameters were used as the default program.

The lowest calculated binding free energies (ΔG^0_b) are tabulated in Table 3 for experimental and theoretical investigations. The binding constant K_b of the complex–receptor has obtained according to the below equation which R is the gas constant and T indicates room temperature in degree Kelvin at the computational results.

$$\Delta G^\circ_b = -RT \ln K_b$$

The binding mode and intermolecular interaction of complex **1** with receptors such as DNA, TrxR 1 and 2 were shown in Figures 4 to 6. The H-bond schemes of the interaction between the complex **1** and receptors in the active site were also shown as well as. It can be seen, H-bond acceptors and donors with a range of colors. For the better understanding type of interactions,

Metallomics Accepted Manuscript

View Article Online
DOI: 10.1039/C9MT00304E

Published on 03 March 2020. Downloaded by University of Canterbury - Christchurch on 3/3/2020 12:19:02 PM.

hydrophobic interactions have been presented with colors and two-dimensional view as well as. Similarly, H-bond interactions, which are related to the other interactions between the complex **1** and receptors from the active site, including pi-pi stakes, pi-sigma, pi-pi T shaped and van der Waals interactions, were obtained for all active sites.

Table 3. Comparison between experiment and theoretical free energy $\Delta G°$ (kcal·mol^{-1}) and relative binding constant K_b of complex **1** with receptors.

Receptor	$\Delta G°_{theo}$	$\Delta G°_{exp}$	$K_{b\ theo}$	$K_{b\ exp}$
DNA	-6.00	-6.09	6.6×10^4	6.87×10^4
TrxR1	-5.88	-	5.3×10^4	-
TrxR2	-5.09	-	1.2×10^4	-

DNA: The highest mode energy of complex **1** with DNA has been shown in Figure 2, which has an excellent presentation for major groove interaction. Ligplot $^+$ software shows a two-dimensional interaction in Figure 4.b as well as. There is one hydrogen bond between the nitrogen atoms of complex **1** by oxygen atom of the adenine base of DNA with 3.24 Å lengths. This bond has been indicated by a green dash line in Figure 4.b. In addition, hydrophobic interactions have been shown Figures 4*c* and *d* in the active binding site of DNA. It can be seen that the hydrophobic interactions are major interaction for this active mode. Many Bases have more than a hydrophobic role in the docked position.

Metallomics Accepted Manuscript

View Article Online
DOI: 10.1039/C9MT00304E

Published on 03 March 2020. Downloaded by University of Canterbury - Christchurch on 3/3/2020 12:19:02 PM.

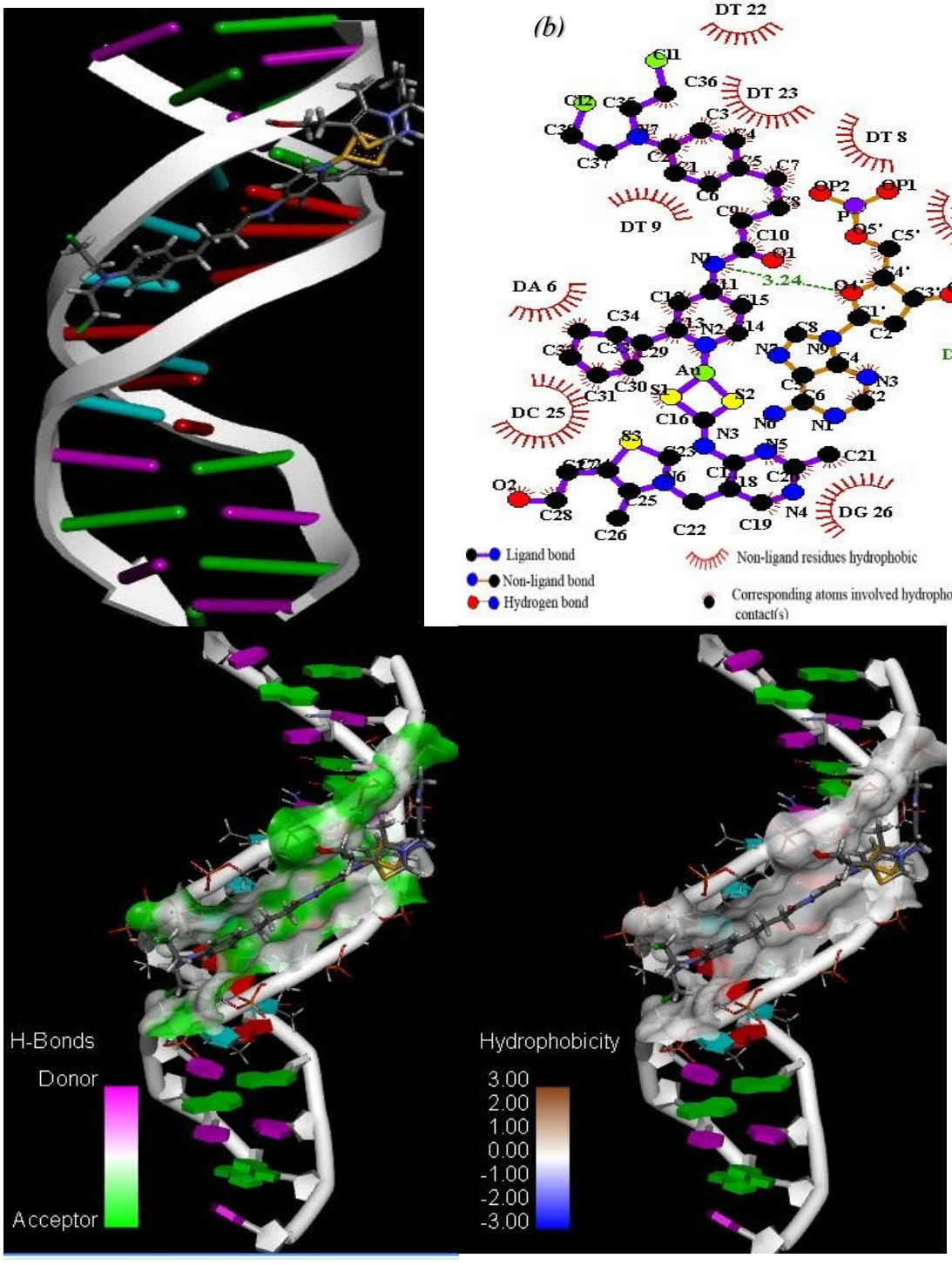

Metallomics Accepted Manuscript

View Article Online
DOI: 10.1039/C9MT00304E

Published on 03 March 2020. Downloaded by University of Canterbury - Christchurch on 3/3/2020 12:19:02 PM.

Figure 4. (a) the complex **1** is docked in the active site of DNA with interaction main bases also (b) 2-D view of the bases of DNA with dominant interactions. H-bond and hydrophilicity ratio presentation complex **1** with DNA in the active site have been shown in the (c) and (d), respectively.

TrxR1 study: The best mode interaction with the key amino acid residues at the active site of TrxR1 with complex **1**, type of interactions and H-bond presentation have been shown in Figure 5. For a better understanding of interactions, two and three views of main residues in the docked pose were investigated. An active site is the part of TrxR1 that directly binds to complex **1**. This active site involved residues, such as Asp 417, His239, Gln 78, Ser 415, His 243, Ala 495, Gly 496, Gly 499, Asn 419, Pro 34 and Arg 416 interactin with complex **1**. It can be seen, there are three hydrogen bonds between the complex **1** with amino acids of TrxR1. Figure 5.d shows that schematic representation of hydrogen bonds with bond lengths of 2.27, 2.96, and 3.02 Å. One of the hydrogen bonds between the oxygen of complex **1** with the nitrogen of Asp418, which has been indicated by a green dash line with 2.27 Å bond length in (see Figure 5.d). There is a major interaction that is hydrophobic, which has been presented as well as. Results show that TrxR1 has better interaction with complex **1** which some good agreements with the inhibition of the TrxR activity due to interaction with complex **1** as viewpoints experimentally and theoretically. Table 3 shows that binding free energy of interaction TrxR1 with complex **1** is more than TrxR2. Both experimental and theoretical studies showed that complex **1** has the strong ability to inhibit TrxR1 in comparison with TrxR2.

Metallomics Accepted Manuscript

View Article Online
DOI: 10.1039/C9MT00304E

Published on 03 March 2020. Downloaded by University of Canterbury - Christchurch on 3/3/2020 12:19:02 PM.

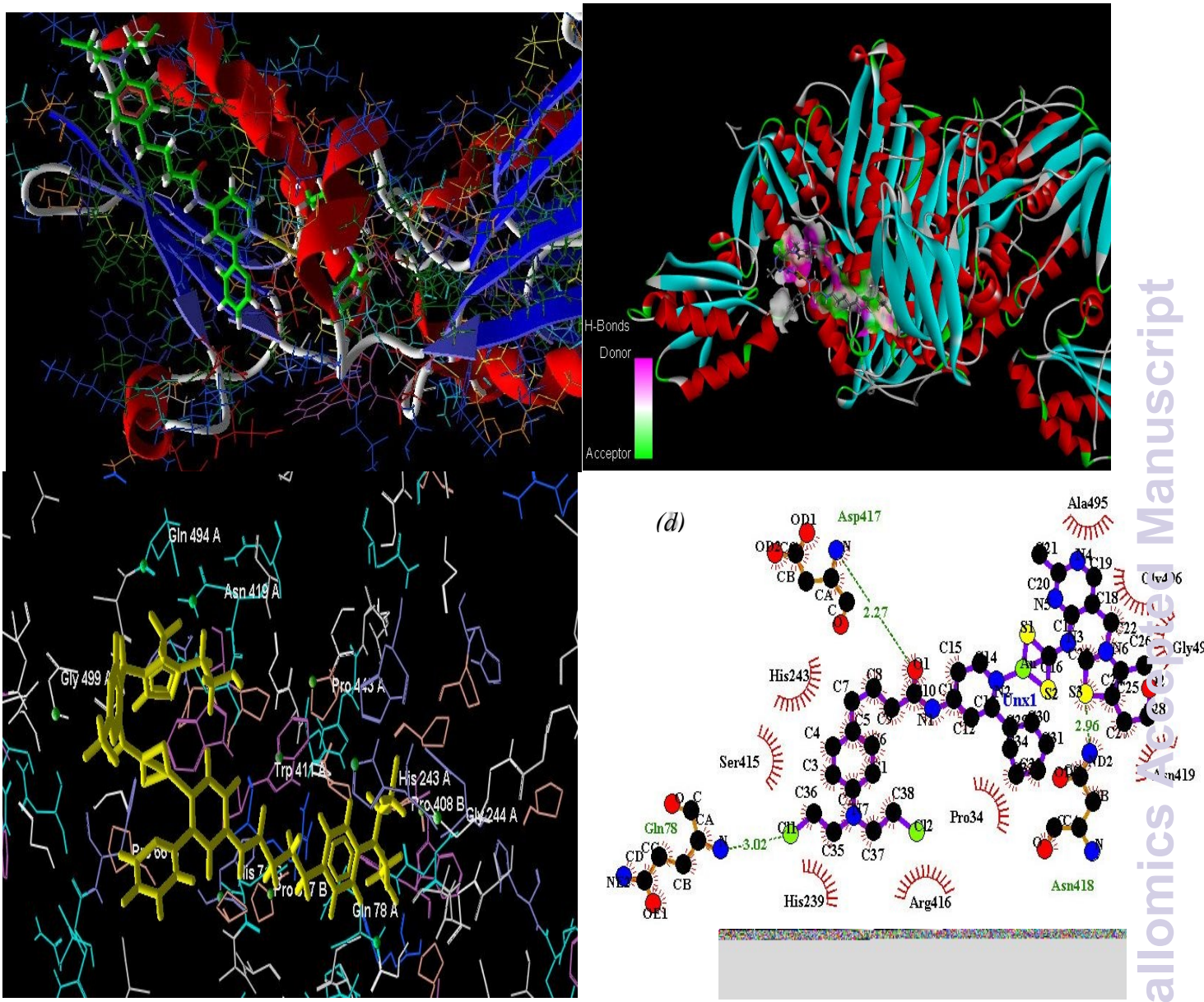

Figure 5. (a) Docking pose of the energy-minimized structure of complex **1** with Asp 417,His239, Gln 78, Ser 415, His 243, Ala 495, Gly 496, Gly 499, Asn 419, Pro 34 and Arg 416 in the active site of TrxR1 also different residues were indicated by specific colors. (b) The main H-bond interaction complex **1** with the amino acids of TrxR1 in the active mode was shown. All interaction types between complex **1** and TrxR1 residues in the active site with three *(c)* and *(d)* two views.

Metallomics Accepted Manuscript

View Article Online
DOI: 10.1039/C9MT00304E

Published on 03 March 2020. Downloaded by University of Canterbury - Christchurch on 3/3/2020 12:19:02 PM.

TrxR2 study:

As it can be seen in Figure 6, all type of interaction complex **1** with residues of TrxR2 were indicated at 2-D and 3 views. As mentioned before, the best energy of interaction and binding constant have been indicated in Table 3. This result has been compared with experimental value and a good agreement was observed. For a better understanding of interaction, active site with the type of interactions was presented in the three and a two-dimensional schemes in Figures 5 *c* and *d*. This active site was defined by the amino acid residues surrounding the bound complex **1**. Lys 107, Lys 97, Gln 89, Lys 80, Leu 110, Phe 78, TRp 81, Lys 123, Gln 88, Thr 90 and 86 are amino acids in the TrxR2 Active site. It can be seen, there is one hydrogen bond between the complex **1** and Thr 86 (Threonine amino acid) with bond length 2.94 Å.

Finally, based on the results can be decided that hydrophobic interactions are as major interactions in the active site for interaction with TrxR2. Also, TrxR1 has better interaction with complex **1**, which is a good agreement with experimental values.

Metallomics Accepted Manuscript

View Article Online
DOI: 10.1039/C9MT00304E

Published on 03 March 2020. Downloaded by University of Canterbury - Christchurch on 3/3/2020 12:19:02 PM.

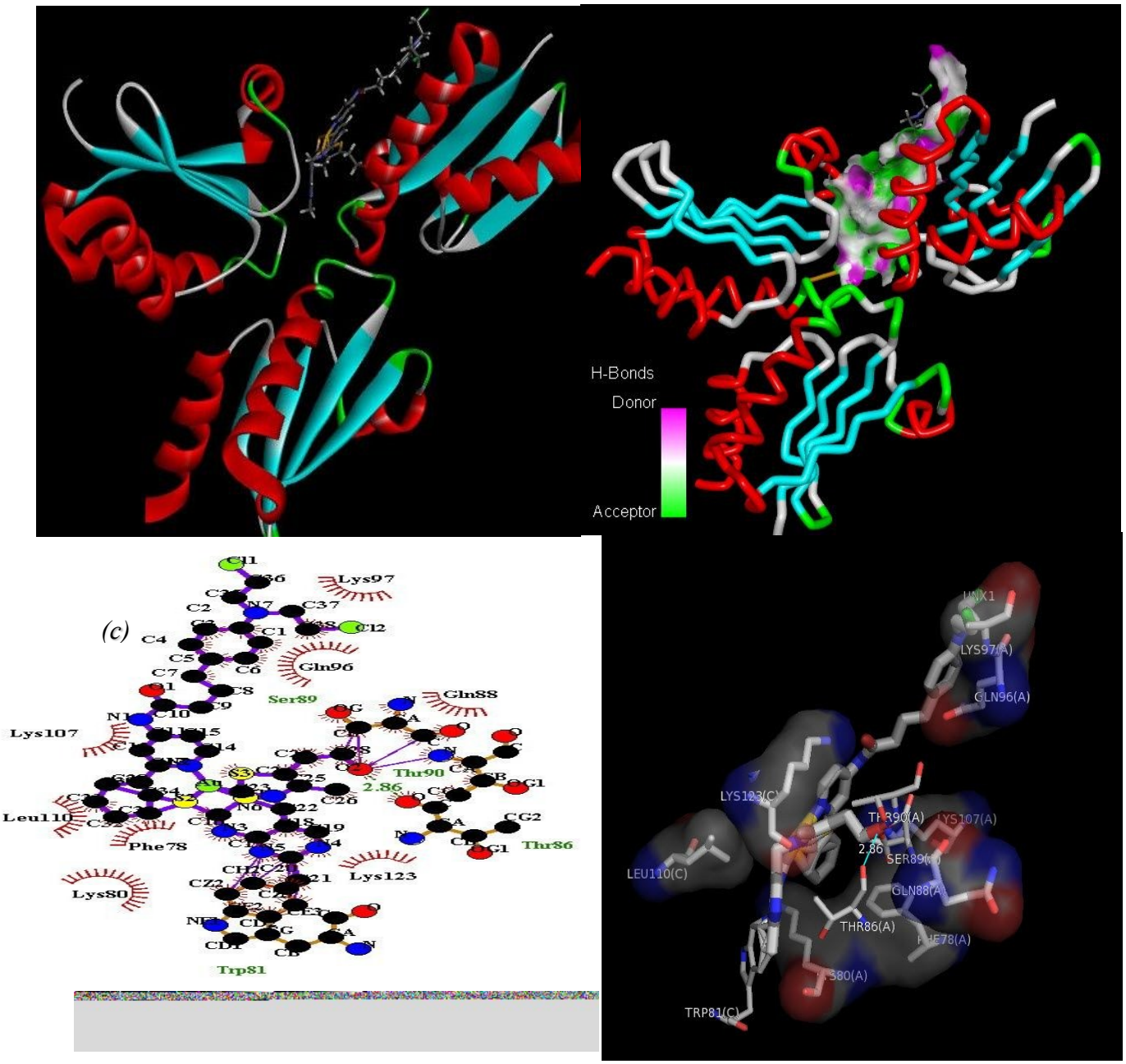

Figure 6. (a) the best docking pose of complex **1** with the residues of TrxR2 with hydrophobicity ratio. (b) The main H-bond interaction complex **1** with the amino acids of TrxR2 was shown. All interaction types between complex **1** and Lys 107, Lys 97, Gln 89, Lys 80, Leu 110, Phe 78, TRp 81, Lys 123, Gln 88, Thr 90 and 86 of TrxR2 residues in the active site by *(c)* three and *(d)* two-dimensional presentations.

Metallomics Accepted Manuscript

View Article Online
DOI: 10.1039/C9MT00304E

Published on 03 March 2020. Downloaded by University of Canterbury - Christchurch on 3/3/2020 12:19:02 PM.

Molecular Orbital calculations

There are four cases for shapes of High Occupied Molecular Orbital (HOMO) and Low Unoccupied Molecular Orbital (LUMO) of complex **1** which have been shown in the Figure S15, as well as. These shapes have also been calculated with the previous method and basis sets in the Gaussian 09 software. Here, the effect of different interactions on the complex **1** has been studied by orbital molecular shapes. Change of receptors because that density of electron will be change so the shape of HOMO and LUMO are different. Case (a) is free complex **1** which optimized in the gas phase then the molecular orbital study has carried out. In this case, HOMO is mostly localized on the Au and S atoms and phenlypridine moiety but its LUMO is more on the phenyl ring of phenlypridine moiety. Shapes of HOMO and LUMO in the deforming complex after interaction with different receptors have been presented in Figures S15-b to S15-d. A comparison of the case (*a*) with (*b*) shows that the change in the HOMO of complex **1** after interaction with DNA is observable. Different between HOMO in the two cases is because of the effect of the receptor. Distribution of density of electrons for case (b) is more localized on the Au, sulfur atoms, phenlypridine, and amine of vitamin B1 moiety. This effect does not observe in the LUMO of complex **1** because it is nearly localized on the vitamin B1 moiety. Generally, HOMO is mostly localized on the phenlypridine moiety, Au, and S atoms in three cases. It is seen that the effect of the interaction complex **1** with TrxR1 on the molecular orbital is different and some part of chlorambucil has a role in the HOMO. In addition, the density of electron of Au atom is more than two previous cases. But, LUMO closer dispersed on vitamin B1 part of complex **1**, Au and sulfur atoms. It evidences that interaction with TrxR1 causes the density of electron distribution localized only on the vitamin B1 part of the molecule so phenlypridine, in this case, does not role in the shape of LUMO. It may be happened because of three strong

Metallomics Accepted Manuscript

View Article Online
DOI: 10.1039/C9MT00304E

Published on 03 March 2020. Downloaded by University of Canterbury - Christchurch on 3/3/2020 12:19:02 PM.

hydrogen bonds between atoms of complex **1** with amino acids of TrxR1. Also, a comparison between case (c) and (d) shows that molecular orbital is more than localized on the Au, sulfur atoms and phenlypridine part. Therefore it can be interpreted that the interaction of TrxR1 is weaker than TrxR1. The shape of molecular orbital for case (d) is near the same of free complex **1** so it can be seen that interaction TrxR2 does not have more effect on the distribution of density of electron of complex **1**.

3. Conclusions

A novel class of cyclometalated gold(III) complex of the type [(CHL-N^C)Au^{III}(B1-DTC)](Cl_2), **1**, that CHL-N^C: chlorambucil coupled with phenylpyridine (CHL-N^C) and B1-DTC: hybrid of vitamin B1 with dithiocarbamate, has been designed and synthesized. The water soluble gold(III) complex has been examined for its antiproliferative effects against breast adenocarcinoma (MCF-7 and MDA-MB-231) and human colon cancer (HCT-116) as well as non-tumorigenic cells human lung fibroblasts (MRC-5). The free ligands were less active with $IC_{50} > 30$ μM in all breast and colon cancer cell lines. However, the complex **1** was 14.5, 12.41, 12.60 times higher than that of cisplatin towards MCF-7, MDA-MB-231 breast cancer, and HCT-116 colon cancer, respectively, with IC_{50} range value 0.43-2.12 μM. Furthermore, the complex **1** was less active in the healthy cell (non-tumorigenic cells, MRC-5) with selectivity index values about 11.87 times greater than cisplatin. The experimental and docking study showed the groove binding of complex **1** with CT DNA. The docking studies showed that the complex is more sensitive to the TrxR relative to the DNA. Therefore, the complex mainly interacts with the TrxR and its biological activity may be consequently TrxR inhibition compare to DNA interaction. Both experimental and theoretical studies showed that complex **1** inhibits the TrxR1 more than TrxR2 and is about 6.43 and 2.56 fold more active than auranofin in

Metallomics Accepted Manuscript

View Article Online
DOI: 10.1039/C9MT00304E

Published on 03 March 2020. Downloaded by University of Canterbury - Christchurch on 3/3/2020 12:19:02 PM.

inhibiting TrxR1 and TrxR2, respectively. Also, TrxR activity in MCF-7 cells showed that complex **1** inhibited TrxR activity 1.74 times more than auranofin and about 73.42% in comparison to TrxR activity in control cells. The apoptosis study of complex **1** showed 77.02% and 5.38% of the MCF-7 cells were in the early and late apoptotic phase, respectively. This observation showed the induced cell death through apoptosis. Overall, these studies document the importance of a new scaffold of gold(III) complex with the conjugation of vitamin B1 and the chemotherapy medication chlorambucil derivatives for the biological properties of the class of cyclometalated Au(III) complexes as anticancer drugs.

Corresponding Author

*E-mail: leila.tabrizi@nuigalway.ie (Leila Tabrizi)

*E-mail: F.abyar@ardakan.ac.ir (Fatemeh Abyar)

ORCID

Leila Tabrizi: 0000-0002-3699-5869

Fatemeh Abyar; 0000-0003-0915-1529

Acknowledgments

The authors would like to thank from the Ardakan University for financial support and the School of Chemistry, National University of Ireland (NUI), Galway for general support. We are grateful for financial support from the Ardakan University.

Notes

All authors declare no conflict of interest.

References

1 S. Spreckelmeyer, C. Orvig, A. Casini, A. *Molecules* 2014, **19**, 15584–15610.

Metallomics Accepted Manuscript

View Article Online
DOI: 10.1039/C9MT00304E

Published on 03 March 2020. Downloaded by University of Canterbury - Christchurch on 3/3/2020 12:19:02 PM.

2 D. Cappetta, F. Rossi, E. Piegari, F. Quaini, L. Berrino, K. Urbanek, A. A. De, *Pharm. Res.* 2018, **127**, 4–14.

3 L. Galluzzi, I. Vitale, J. Michels, C. Brenner, G. Szabadkai, A. Harel-Bellan, M. Castedo, G. Kroemer, *Cell Death Dis.* 2014, **5**, e1257.

4 S. Dilruba, G. V. Kalayda, *Cancer Chemother. Pharm.* 2016, **77**, 1103–1124.

5 T. Lazarevic, A. Rilak, Z. D. Bugarcic, *Eur. J. Med. Chem.* 2017, **142**, 8–31.

6 J. J. Soldevila-Barreda, P. J. Sadler, *Curr. Opin. Chem. Biol.* 2015, **25**, 172–183.

7 C. Nardon, D. Fregona, *Curr. Med. Chem.* 2018, **25**, 434–436.

8 A. Casini, R. W. Sun, I. Ott, *Met. Ions Life Sci.* 2018, **18**. doi: 10.1515/9783110470734-013.

9 B. Bertrand, M. R. M. Williams, M. Bochmann, *Chem.: Eur. J.* 2018, **24**, 11840–11851.

10 M. Celegato, C. Borghese, N. Casagrande, M. Mongiat, X. U. Kahle, A. Paulitti, M. Spina, A. Colombatti, D. Aldinucci, *Blood* 2015, **126**, 1394–1397.

11 D. Aldinucci, D. Lorenzon, L. Stefani, L. Giovagnini, A. Colombatti, D. Fregona, *Anticancer Drugs* 2007, **18**, 323–332.

12 V. Milacic, D. Chen, L. Ronconi, K. R. Landis-Piwowar, D. Fregona, Q. P. Dou, *Cancer Res.* 2006, **66**, 10478–10486.

13 P. Gratteri, L. Massai, E. Michelucci, R. Rigo, L. Messori, M. A. Cinellu, C. Musetti, C. Sissi, C. Bazzicalupi, *Dalton Trans.* 2015, **44**, 3633–3639.

14 M. Coronnello, G. Marcon, S. Carotti, B. Caciagli, E. Mini, T. Mazzei, P. Orioli, L. Messori, *Oncol Res.* 2000, **12**, 361–370.

15 D. Saggioro, M. P. Rigobello, L. Paloschi, A. Folda, S. A. Moggach, S. Parsons, L. Ronconi, D. Fregona, A. Bindoli, *Chem. Biol.* 2007, **14**, 1128–1139.

Metallomics Accepted Manuscript

View Article Online
DOI: 10.1039/C9MT00304E

Published on 03 March 2020. Downloaded by University of Canterbury - Christchurch on 3/3/2020 12:19:02 PM.

16 Mendes, F.; Groessl, M.; Nazarov, A. A.; Tsybin, Y. O.; Sava, G.; Santos, I.; Dyson, P. J.; Casini, A. Metal-Based Inhibition of Poly(ADP-ribose) Polymerase − The Guardian Angel of DNA. *J. Med. Chem.* **2011**, *54*, 2196−2206.

17 T. Zou, C. T. Lum, C.-N. Lok, J.-J. Zhang, C.-M. Che, *Chem. Soc. Rev.* 2015, **44**, 8786--8801

18 M. Coronnello, E. Mini, B. Caciagli, M. A. Cinellu, A. Bindoli, C. Gabbiani, L. Messori, *J. Med. Chem.* 2005, **48**, 6761–6765.

19 R. W.-Y. Sun, C.-N. Lok, T. T.-H. Fong, C. K.-L. Li, Z. F. Yang, T. Zou, A. F.-M. Siu, C.-M. Che, *Chem. Sci.* 2013, **4**, 1979–1988.

20 B. Bertrand, M. Bochmann, J. Fernandez-Cestau, L. Rocchigiani, in Pincer Compounds – Chemistry and Applications, ed. D. Morales-Morales, Elsevier, Amsterdam, 2018, ch. 31, 673–699.

21 R. V. Parish, B. P. Howe, J. P. Wright, J. Mack, R. G. Pritchard, R. G. Buckley, A. M. Elsome, S. P. Fricker, *Inorg. Chem.* 1996, **35**, 1659–1666.

22 Y. Zhu, B. R. Cameron, R. Mosi, V. Anastassov, J. Cox, L. Qin, Z. Santucci, M. Metz, R. T. Skerlj, S. P. Fricker, *J. Inorg. Biochem.* 2011, **105**, 754–762.

23 D. Fan, C.-T. Yang, J. D. Ranford, J. J. Vittal, P. F. Lee, *Dalton Trans.* 2003, 3376–3381.

24 M. Frik, J. Fernandez-Gallardo, O. Gonzalo, V. Mangas- Sanjuan, M. Gonzalez-Alvarez, A. S. del Valle, C. Hu, I. Gonzalez-Alvarez, M. Bermejo, I. Marzo, M. Contel, *J. Med. Chem.* 2015, **58**, 5825–5841.

25 B. Bertrand, J. Fernandez-Cestau, J. Angulo, M. M. D. Cominetti, Z. A. E. Waller, M. Searcey, M. A. O'Connell, M. Bochmann, *Inorg. Chem.* 2017, **56**, 5728−5740.

Metallomics Accepted Manuscript

View Article Online
DOI: 10.1039/C9MT00304E

Published on 03 March 2020. Downloaded by University of Canterbury - Christchurch on 3/3/2020 12:19:02 PM.

26 M. R. M. Williams, B. Bertrand, D. L. Hughes, Z. A. E. Waller, C. Schmidt, I. Ott, M. O'Connell, M. Searcey, M. Bochmann, *Metallomics* 2018, **10**, 1655-1666.

27 B. Bertrand, S. Spreckelmeyer, E. Bodio, F. Cocco, M. Picquet, P. Richard, P. Le Gendre, C. Orvig, M. A. Cinellu, A. Casini, *Dalton Trans.* 2015, **44**, 11911–11918.

28 S. Gukathasan, S. Parkin, S. G. Awuah, *Inorg. Chem.* 2019, **58**, 9326−9340.

29 M. Altaf, N. Casagrande, E. Mariotto, N. Baig, A. N. Kawde, G. Corona, R. Larcher, C. Borghese, C. Pavan, A. A. Seliman, D. Aldinucci, A. A. Isab, *Cancers* 2019, **11**, 474.

30 M. Altaf, M; Monim-ul-Mehboob, A. A. Seliman, M. Sohail, M. I. Wazeer, A. A. Isab, L. Li, V. Dhuna, G. Bhatia, K. Dhuna, *Eur. J. Med. Chem.* 2015, **95**, 464–472.

31 M. Altaf, M. Monim-ul-Mehboob, A. N. Kawde, G. Corona, R. Larcher, M. Ogasawara, N. Casagrande, M. Celegato, C. Borghese, Z. H. Siddik, et al. *Oncotarget* 2017, **8**, 490–505.

32 N. Shaik, A. Martinez, I. Augustin, H. Giovinazzo, A. Varela- Ramirez, M. Sanau, R. J. Aguilera, M. Contel, *Inorg. Chem.* 2009, **48**, 1577–1587.

33 J. J. Zhang, K. M. Ng, C. N. Lok, R. W. Y. Sun, C.-M. Che, *Chem. Commun.* 2013, **49**, 5153–5155.

34 V. Milacic, D. Chen, L. Ronconi, K. R. Landis-Piwowar, D. Fregona, Q. Ping Dou. *Cancer Res* 2006, **66**, 10478-10486.

35 M. R. Caira, G. V. Fazakerley, P. W. Linder, L. R. Nassimbeni, *Acta Cryst.* 1974, **B30**, 1660-1666.

36 R. E. Cramer, R. B. Maynard, J. A. Ibers, *J. Am. Chem. Soc.* 1981, **103**, 76–81.

37 R. E. Cramer, R. B. Maynard, R. S. Evangelista, *J. Am. Chem. Soc.* 1984, **106**, 111–116.

38 R. E. Cramer, R. E. Kirkup, M. J. J. Carrie, *Inorg. Chem.* 1988, **27**, 123-130.

Metallomics Accepted Manuscript

View Article Online
DOI: 10.1039/C9MT00304E

Published on 03 March 2020. Downloaded by University of Canterbury - Christchurch on 3/3/2020 12:19:02 PM.

39 A. Bencini, E. Borghi, *Inorg. Chim. Acta* 1987, **135**, 85–91.

40 R. Bau, Y. S. Hyun, J. Lim, H. K. Choi, A. Yannopoulos, N. Hadjiliadis, *Inorg. Chim. Acta* 1988, **150**, 107–112.

41 E. Archibong, A. Adeyemo, K. Aoki, H. Yamazaki, *Inorg. Chim. Acta* 1989, **156**, 77–83.

42 J. S. Casas, E. E. Castellano, M. D. Couce, A. Sánchez, J. Sordo, J. M. Varela, J. Zukerman-Schpector, *Inorg. Chem.* 1995, **34**, 2430–2437.

43 N. H. Hu, T. Norifusa, K. Aoki, *Polyhedron* 1999, **18**, 2987–2994.

44 K. Aoki, N. H. Hu, H. Yamazaki, A. O. Adeyemo, *Inorg. Chim. Acta* 1990, **175**, 247–254.

45 N. H. Hu, K. Aoki, A. O. Adeyemo, G. N. Wiliams, *Inorg. Chim. Acta* 2001, **325**, 9–19.

46 J. S. Casas, A. Castineras, M. D. Couce, A. Sánchez, J. Sordo, J. M. Varela, *Polyhedron* 1995, **14**, 1825–1829.

47 N. H. Hu, K. Aoki, A. O. Adeyemo, G. N. Williams, *Inorg. Chim. Acta* 2001, **325**, 9–19.

48 K. Dodi, I. P. Gerothanassis, N. Hadjiliadis, A. Schreiber, R. Bau, I. S. Butler, P. J. Barrie, *Inorg. Chem.* 1996**, 35**, 6513–6519.

49 K. Aoki, H. Yamazaki, *J. Am. Chem. Soc.* 1980, **102**, 6878–6880.

50 G. Malandrinos, M. Louloudi, A. I. Koukkou, I. Sovago, C. Drainas, N. Hadjiliadis, *J. Bio. Inorg. Chem.* 2000, **5**, 218–226.

51 J. S. Casas, E. E. Castellano, M. D. Couce, J. Ellena, A. Sánchez, J. Sordo, C. Taboada, *J. Inorg. Biochem.* 2006, **100**, 124–132.

52 N. H. Hu, T. Tokuno, K. Aoki, *Inorg. Chim. Acta* 1999, **295**, 71–83.

53 P. Brandão, S. Guieu, A. Correia-Branco, C. Silva, F. Martel, *Inorg. Chim. Acta* 2019, **487**, 287–294.

Metallomics Accepted Manuscript

View Article Online
DOI: 10.1039/C9MT00304E

Published on 03 March 2020. Downloaded by University of Canterbury - Christchurch on 3/3/2020 12:19:02 PM.

54 H. Myrberg, L. Zhang, M. Mäe, U. Langel, *Bioconjugate Chem.* 2008, **19**, 70–75.

55 M. Mäe, H. Myrberg, S. El-Andaloussi, U. Langel, *Int. J. Pept. Res. Ther.* 2009, **15**, 11–15.

56 S. B. Fonseca, S. O. Kelley, *ACS Med. Chem. Lett.* 2011, **2**, 419–423.

57 J. Hoyer, U. Schatzschneider, M. Schulz-Siegmund, I. Neundorf, *Beilstein J. Org. Chem.* 2012, **8**, 1788–1797.

58 X. Qin, L. Fang, F. Chen, S. Gou, *Eur. J. Med. Chem.* 2017, **137**, 167–175.

59 R. K. Pathak, R. Wen, N. Kolishetti, S. Dhar, *Mol. Cancer Ther.* 2017, **16**, 625–636.

60 D. Montagner, D. Tolan, E. Andriollo, V. Gandin, C. A. Marzano, *Int. J. Mol. Sci.* 2018, **19**, 3775.

61 L. Tabrizi, L.O. Olasunkanmi, O. A. Fadare, *Chemical Communications,* 2019, DOI: 10.1039/C9CC07406F

62 H. L. M. Van Gaal, J. W. Diesveld, F. W. Pijpers, F. W.; J. G. M. Van der Linden, *Inorg. Chem.* 1979, **18**, 3251-3260.

63 L. Tabrizi, F. Abyar, *Mol. Pharmaceutics* 2019, **16**, 3802−3813.

64 S. Radisavljević, D. Ćoćić, S. Jovanović, B. Šmit, M. Petković, N. Milivojević, N.; Planojević, S. Marković, B. Petrović, *JBIC J. Biol. Inorg. Chem.* 2019, **24**, 1057–1076.

65 V. Rodríguez-Fanjul, E. Lopez-Torres, M. Antonia Mendiola, A. María Pizarro, *Eur. J. Med. Chem.* 2018, **148**, 372-383.

66 J. Lu, E.-H. Chew, A. Holmgren, *Proc Natl Acad Sci USA*, 2007, **104(30)**, 12288-12293.

67 Y. Ouyang, Y. Peng, J. Li, A. Holmgren, J. Lu, *Metallomics* 2018,**10(2)**, 218-228.

Metallomics Accepted Manuscript

View Article Online
DOI: 10.1039/C9MT00304E

Published on 03 March 2020. Downloaded by University of Canterbury - Christchurch on 3/3/2020 12:19:02 PM.

68 V. Gandin, A. P. Fernandes, M. P. Rigobello, B. Dani, F. Sorrentino, F. Tisato, M. Bjornstedt, A. Bindoli, A. Sturaro, R. Rella and C. Marzano, *Biochemical pharmacology*, 2010, **79**, 90-101.

69 http://www.rcsb.org/structure/5ZLD

70 K. Fritz-Wolf, S. Kehr, M. Stumpf, S. Rahlfs, K. Becker, *Nat. Commun.* 2011, **2**, 383.

71 M. Peng, D. Cascio, P. F. Egea, *Biochem. Biophys. Res. Commun.* 2015, 456, 403-409.

72 http://www.rcsb.org.

73 A. W. Ghoorah, M. Smail-Tabbone, M.-D. Devignes, D. W. Ritchie, *Bioinformatics.* 2013, **81**, 2150–2158.

74 H. Park, J. Lee, S. Lee, P*roteins: Struct. Funct. Bioinf.* 2006, **65**, 549-554.

75 R. S. Judson, E. P. Jaeger, A, M. Treasurywala. *J. Mol. Struc.-Theochem.* 1994, **308**, 191-206.

Metallomics Accepted Manuscript